Processing data from the SPIRE imaging Fourier transform spectrometer

SPIRE-BSS-NOT-002664

Blue Sky Spectroscopy Inc.

Peter Davis

version 1.0
13 June 2006

Processing data from the SPIRE imaging Fourier transform spectrometer

Blue Sky Spectroscopy Inc.
Peter Davis

Table of Contents

Chapter 1. Preface

1.1. Acknowledgements

Trevor Fulton and Jamil Shariff reviewed an earlier draft of this document which helped improve it considerably. Shannon MacLeod set up the docBook infrastructure. Funding for this note was provided by the Canadian Space Agency.

1.2. Scope

This document introduces data processing for the SPIRE imaging spectrometer. After briefly discussing (imaging) Fourier transform spectroscopy more generally (Chapter 2, *Fourier transform spectroscopy*) and its requirements for data processing (Chapter 3, *Data Processing for FTS*), it describes data processing requirements specific to the SPIRE spectrometer (Chapter 4, *The SPIRE imaging FTS*).

1.3. Acronyms

Table 1.1. Acronyms used in this document

Acronym	**Long-hand**
CS	Continuous scan
iFTS	Imaging Fourier transform spectrometer
FFT	Fast Fourier transform
FT	Fourier transform
FTS	Fourier transform spectrometer
LVDT	Linear variable displacement transducer
OPD	Optical path difference
PCF	Phase correction function
PID	Proportional, integral, and derivative control
SCal	Spectrometer calibration source
SI	Step and integrate
SPIRE	Spectral and photometric imaging receiver
ZPD	Zero Path Difference

Chapter 2. Fourier transform spectroscopy

2.1. Basics of Fourier transform spectroscopy

The optical design of a Fourier transform spectrometer (FTS) can be kept very simple: Mirrors and beamsplitters are used to divide the incoming light into two beams, send them along two arms, and recombine the two beams again. A moving mirror changes the path length of one of the beams, thereby modulating the optical path difference (OPD) between the two arms of the spectrometer. The recombining beams lead to an interference pattern (fringes) at the focus: the interferogram (see Figure 2.1, “A sample interferogram, centered around the central burst; intensity versus OPD in arbitrary units.”). The spectral resolution of a given system depends on the maximum possible OPD modulation: the larger the maximum OPD of an FTS system the better its spectral resolution. The optical design for imaging FTS (iFTS) systems is identical, adding the complexity to take into account image quality. Zero path difference (ZPD) is a unique point of symmetry of the FTS system, where the path lengths of the two beams are identical and radiation of all wavelengths interferes constructively, leading to a very bright central maximum of the interference pattern (for a thorough introduction to FTS see [Davis et al. 2001]).

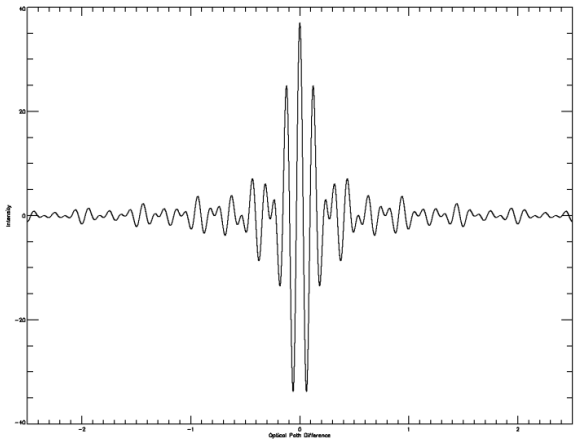

Figure 2.1. A sample interferogram, centered around the central burst; intensity versus OPD in arbitrary units.

An FTS can operate in two different modes: The Continuous Scan (CS) mode keeps the moving mirror at a constant speed while continuously recording the interferogram. The Step and Integrate (SI) mode moves the mirror to target positions and measurements are taken while this mirror is stationary at that position. The CS mode is the baseline for the SPIRE iFTS.

2.2. System Configurations

The *Michelson* FTS is the most straightforward configuration of an FTS (see Figure 2.2, “The optical layout of an (imaging) FTS in Michelson configuration.”). It employs plane mirrors and one beamsplitter to direct the light from the input port into two beams. The path length of one beam is fixed and the path length of the other beam can be adjusted by moving a reflecting mirror which is placed on a linear translation stage. The two beams are recombined through the same beamsplitter which divides the incoming light. The modulated OPD between the two beams leads to an interference pattern at the focal plane as a function of OPD.

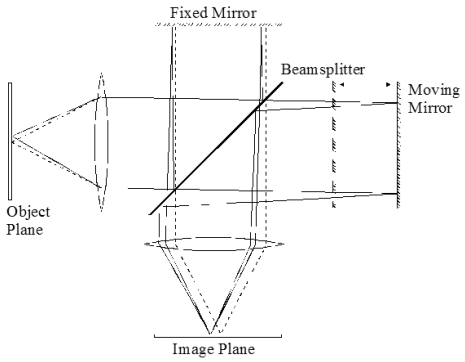

Figure 2.2. The optical layout of an (imaging) FTS in Michelson configuration.

The *Mach-Zehnder* configuration of an FTS employs two beamsplitters giving access to two input and two output ports (see Figure 2.3, “The optical layout of an (imaging) FTS in Mach-Zehnder configuration.”). The difference between the path lengths of the two beams is modulated by moving several components of the system.

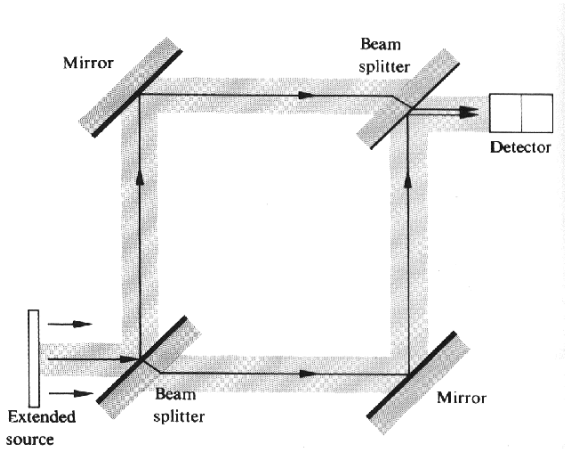

Figure 2.3. The optical layout of an (imaging) FTS in Mach-Zehnder configuration.

The SPIRE interferometer is of the Mach-Zehnder variety, following a design from [Ade et al. 1999] (see Figure 2.4, “(An early draft of) The optical layout of the interferometer of the SPIRE imaging FTS.”). Powered mirrors fold the two beams towards the line of symmetry so that the optical path difference is modulated by a single linear translation stage mechanism. The stage mechanism carries two back-to-back rooftop mirrors. A displacement of Δx of the mechanism shortens one beam path by $2 \cdot \Delta x$ and lengthens the other beam path by $2 \cdot \Delta x$, leading to an overall modulation of $\Delta_{OPD} = 4 \cdot \Delta x$. Such a compact design is particularly well suited for deployment in space.

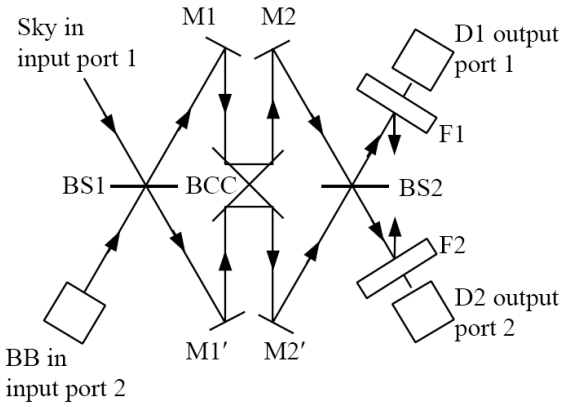

Figure 2.4. (An early draft of) The optical layout of the interferometer of the SPIRE imaging FTS.

2.3. Component design

FTS systems employ components commonly used in optical instrumentation: Mirrors and beamsplitters. The engineering challenge for optical components lies in manufacturing a beamsplitter to divide the beam into two beams of equal intensity. Beamsplitters are commonly distinguished into polarizing and intensity beamsplitters depending on whether they separate radiation depending on its polarization or not. The specific choice for a given instrument depends on the targeted spectral range of the instrument. SPIRE uses broad-band, intensity beamsplitters.

Mechanically, the most difficult aspect of an FTS is the linear translation stage. The longest throw of the linear stage sets physical limits for the best resolution possible with an FTS. The smallest resolution element $\Delta\sigma$ of an FTS is given by: $\Delta\sigma = 1 / (2 \cdot OPD_{max})$

The engineering challenge for the stage is to control it to a very high precision: either the stage must be kept at a constant speed, usually employing PID control systems, or it must move in precisely equidistant steps of an order below the shortest wavelength observed. A metrology system for the translation stage must be in place for the PID control and to record the positions of the stage. SPIRE employs two metrology systems: An optical encoder determines relative changes of the position of the stage to an accuracy of 1 μm through the whole range of the stage translation. An interpolation algorithm provides spatial information to a precision of ~ 10 nm. An LVDT gives absolute position measurements of an accuracy of ~ 100 nm close to ZPD.

In the case of SPIRE, the maximum OPD modulation possible is $4 \cdot \sim 3.5$ cm = ~ 14 cm and the resulting resolution element is ~ 0.036 cm^{-1}. The best achievable resolution of an FTS is slightly larger than the resolution element as the full width of the instrumental line shape at half maximum is widened by a factor of 1.207, which brings the best resolution of SPIRE to ~ 0.043 cm^{-1}.

2.4. Detection

An FTS produces an interference pattern at the focal plane which is measured with single pixel detectors or detector arrays in the case of an iFTS. The interferogram I(x) is defined as the power measured at an output port of an FTS as a function of OPD. A computer records an (array of) interferogram(s) via read-out electronics. According to the Nyquist sampling criterion, at least two sample points must be available for the shortest measured wavelength. If possible, FTS systems are over-sampled by a factor of 2-4 to recover from lost or invalid data samples. The OPD interval Δ_{OPD}, at which samples are taken, defines the maximum or Nyquist frequency that can be recorded with the FTS. The Nyquist frequency is given by: $\sigma_{Ny} = 1 / (2 \cdot \Delta_{OPD})$

SPIRE cannot provide detector readings at a constant OPD interval. Instead, SPIRE reads out data

from the stage and the detector arrays at constant time intervals (see Section 4.1, “Interpolation”). The detector arrays are read out at a rate of ~ 80 Hz which, with a nominal stage speed of v_{OPD} = 2 mm/s, leads to a nominal sampling interval of 25μm. SPIRE is approximately fourfold oversampled under nominal operating conditions with a Nyquist frequency of ~200 cm^{-1} and an instrumental sensitivity out to ~50 cm^{-1}, corresponding to the shortest observable wavelength of 200 μm.

Chapter 3. Data Processing for FTS

Interferograms, the raw data from FTS systems, have only little intuitive bearing to the measured spectrum. Some fundamental processing steps have to be carried out in order to produce a spectrum. Careful data processing is required to derive accurate spectrometry.

3.1. Fourier Transformation

A Fourier transform (FT) has to be applied to convert the interferogram I(OPD) into a spectrum B(σ). It is defined as follows:

$$F(\sigma) = FT(f(x)) = \sum_{x=-infinity}^{+infinity} f(x) \exp(- i 2\pi \sigma x)$$

$$f(x) = FT^{-1}(F(\sigma)) = \sum_{x=-infinity}^{infinity} F(\sigma) \exp(i 2\pi \sigma x)$$

The FT is the minimal core processing step for any processing of FTS data. The computational complexity of the discrete FT is of the order of $O(n^2)$ because for each sample point, a sum across all other sample points has to be calculated. In the 60's, a Fast FT (FFT) algorithm was developed (see [Cooley Tukey 1965]) which reduces the computational complexity to O(n log(n)). This is a considerable performance improvement over the straightforward discrete FT. Further performance improvements have been integrated into state-of-the-art FFT code (see for example [Frigo Johnson 2005]). Note that standard FFT packages make the assumption that Fourier samples are available at equidistant intervals.

3.2. Instrumental Line Shape

The discrete FT assumes a sum over an infinite number of Fourier components which are supplied from modulating OPD and recording the resulting intensities at the focal plane. Clearly, the OPD of real systems cannot reach from negative to positive infinity. As noted above during the discussion of the linear translation stage, the OPD range is limited by its physical dimensions. The truncation of the interferogram due to the finiteness of the system corresponds to the multiplication of the infinitely extending interferogram with a top-hat function which is unity where samples are available and zero otherwise. This multiplication in the interferogram domain equals a convolution of the spectrum with the sinc-function sinc(x) = sin(x)/x (see Figure 3.1, “The full width of the ideal, instrumental line shape of an FTS; intensiy in arbitrary units versus wavenumber.”), which is the FT of the top-hat function. This truncation of the infinitely extending interferogram defines the instrumental line shape of an FTS which will present itself whenever an FTS measures an unresolved line. While an FTS is limited in the achievable resolution by the physical dimensions of the instrument, the instrumental line shape and its impact on the resulting spectra are well defined and can be taken into account when extracting information from the measured spectrum.

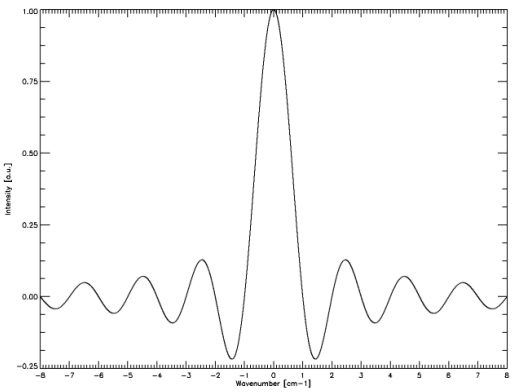

Figure 3.1. The full width of the ideal, instrumental line shape of an FTS; intensiy in arbitrary units versus wavenumber.

3.3. Efficiency Losses

Real FTS systems suffer from an imperfect overlap of the two light beams on recombination, in particular for high OPD. If this efficiency loss is the same regardless of OPD a decrease in the modulation efficiency results. Often, the efficiency losses worsen with increasing OPD leading to a gradual rather than sudden information loss of the infinite Fourier series. A ‘natural apodization’ in the interferogram results. This natural apodization reduces the spectral resolution but also reduces the side-lobes associated with line features – hence the name apodization (greek for 'removing feet'). Natural apodization is often more pronounced for off-axis pixels.

In addition to the natural apodization introduced by the optical layout of the instrument, it is also possible to deliberately simulate such an efficiency loss and multiply the interferogram with an apodization function to trade spectral resolution for a reduction of ringing features. It turns out that there is an optimal boundary to how much spectral resolution has to be sacrificed in order to reduce side-lobes by a given amount. Optimal apodization functions can be derived approaching this boundary (see [Tahic Naylor 2005]).

Similar to the decreased modulation efficiency at high OPD, the overall power received by pixels away from the optical axis decreases towards high OPD. This kind of efficiency loss is called vignetting.

3.4. Phase Correction

The power measured at the focus of an FTS depends strictly on the difference between the optical path lengths of the two beams of the interferometer: the interferogram should be perfectly symmetrical w.r.t. ZPD, which is the unique point where the path lengths of the two beams are identical and constructive interference occurs for all wavelengths. This can be seen easily in the monochromatic case. For a given wavelength λ, destructive interference will occur for the first time where the path difference between the two beams equals $\lambda/2$. Destructive interference occurs, regardless which one of the two beam paths is shorter, at the OPD = $\lambda/2$ to either side of ZPD.

Data must be available on either side of ZPD in order to identify any asymmetries in the interferogram. An interferogram that records data on either side of ZPD is called double-sided. In order to maximize the spectral resolution achievable with an FTS, i.e. in order to maximize OPD_{max}, FTS are designed to record only a short double-sided interferogram while most of the OPD modulation is towards one of the sides. An interferogram that records data on mostly one side of ZPD, is called single-sided. In the case of SPIRE the double-sided interferogram goes out to an OPD ~ 14 mm, or one tenth of the single-sided interferogram which goes up to an OPD ~ 140 mm.

The asymmetries of a double-sided interferogram can be measured by its phase:

$\tan(\Phi(\sigma)) = \text{Imaginary}(FT(I(OPD)) / \text{Real}(FT(I(OPD))$

The spectrum of a purely symmetrical interferogram has no imaginary part (it can be represented as a cosine-transformation) and therefore zero phase. All real FTS systems produce interferograms with non-zero phase. If the phase is linear, then the symmetry of the continuous interferogram is preserved, however the point of symmetry, ZPD, is shifted. Asymmetries in the interferogram derive from various sources:

$$\Phi(\sigma)_{Total} = \Phi(\sigma)_{ZPD} + \Phi(\sigma)_{Optical} + \Phi(\sigma)_{Electrical} + \Phi(\sigma)_{Thermal} + \Phi(\sigma)_{Noise}$$

$\Phi(\sigma)_{ZPD}$: There is no guarantee that a detector sample will be available precisely at ZPD. Any missampling of ZPD by δx leads to an asymmetrical interferogram and a linear phase: $\Phi(\sigma)_{ZPD} = 2\pi\,\delta x\,\sigma$.

$\Phi(\sigma)_{Optical}$: The optical path length may differ for different wavelengths as the refractive index of dielectric media will, in general, depend on wavelength. For SPIRE, the only transmission through dielectrics within the interferometer occurs at the beamsplitters which are known to be the source of non-linear phase.

$\Phi(\sigma)_{Electrical}$: The read-out electronics which convert the analog detector signal into digital, com-

puter-readable format introduce a frequency-dependent phase, which will be, in general, non-linear. The electrical phase can be calculated from the characteristics of the read-out electronics.

$\Phi(\sigma)_{Thermal}$: The detection of electromagnetic radiation is not instantaneous and introduces at least a time-lag (equivalent to a linear phase) and, if detection efficiency differs for different wavelengths, also a non-linear phase. For SPIRE, the thermal behavior of the bolometer crystals is a considerable source of phase error.

$\Phi(\sigma)_{Noise}$: The usual noise sources (photon noise, stage jitter, electrical noise, …) contribute to asymmetries which cannot be avoided.

The knowledge that the interferogram should not have any phase other than noise contributions can be used to develop a phase correction scheme. The idea is to characterize the phase and eliminate the systematic phase from the interferogram, leaving only a noisy phase around zero. The first step is to compute the phase from the double-sided portion of the interferogram. Since the phase is determined by instrument features, it is possible to characterize the phase to a high degree of precision by fitting a curve to the phase and averaging the measured and fitted phase of many double-sided interferograms, thereby eliminating the noise component. The phase from the double-sided interferogram will not provide the phase at the resolution limit of the spectrometer if the double-sided interferogram is shorter than the single-sided interferogram. It is therefore necessary to make the assumption that the shape of the phase can be extrapolated to higher spectral resolution. Once the instrumental phase has been characterized (either from prior calibration measurements or from the individual measurement in question), a phase correction function (PCF) can be defined: $PCF(OPD) = FT^{-1}(\exp(-i \cdot \Phi(\sigma)))$ The phase can then be removed from the interferogram by convolving the interferogram with the PCF: $I_{phasecorrected}(OPD) = I(OPD) \otimes PCF(OPD)$ The phase corrected, single-sided interferogram can then be transformed into a spectrum.

3.5. Deglitching

The detector, while recording the interferogram, may be subject to contaminating influences such as electromagnetic contamination (often the case for noisy operational environments) or high energy particles (space radiation). Contaminating radiation can strike the detector at any time and leads to transient features in the interferograms. These glitches have to be identified and removed in order to avoid artifacts in the resulting spectra. Manual deglitching is feasible for single-pixel FTS. As an imaging FTS with 66 active pixels, SPIRE requires automated deglitching routines.

Chapter 4. The SPIRE imaging FTS

SPIRE is an iFTS for the European Space Agency's Herschel far-infrared and submillimeter observatory ([Swinyard et al. 2003]). Deployment in space introduces specific constraints. Two of these limitations are of particular relevance when processing data from SPIRE:

1. The read-out electronics have to accommodate the limited power and heat budget for a cryogenically cooled instrument for a space mission. Much effort can be spent on triggering a detector read-out when the moving mirror has moved by a given distance for a ground-based FTS, thereby guaranteeing an equidistantly sampled interferogram. Such a synchronization is not feasible given the space environment in which the SPIRE detector read-out electronics have to operate. Detector and stage samples are time-stamped instead. This loss of synchronization has to be accommodated in post-processing.

2. The SPIRE focal plane unit will be cooled to just a few degrees above absolute zero and many of the target sources will be very faint and cold (of the order of a few tens of degrees Kelvin). The Herschel telescope however will be at a temperature of the order of 80 Kelvin which will make it the dominant source of power for all observations. As SPIRE makes a differential measurement of the two input ports, an additional source (SCal) was included in the instrument design to provide compensating power to the second input port. This decreases the dynamic range for the detectors, which, in turn, increases the precision with which detector readings can be taken. Both, the telescope and the SCal emission have to be taken into account during data processing to retrieve the signal from the astronomical source.

4.1. Interpolation

SPIRE's stage mechanism cannot be synchronized with the detector arrays to trigger a read-out after traveling a fixed distance Δ_{OPD}. Put differently: SPIRE cannot guarantee that detector samples are available on an equidistant OPD grid in order to perform an FFT. Instead, stage position OPD(t) and detector data I(t') are read out at ~ 226 Hz and ~ 80 Hz respectively. The time-stamped samples allow an interpolation of the data to an OPD-dependent interferogram I(OPD). This interpolation will lead to a non-equidistant spacing of the detector signals, because the stage speed is not perfectly constant. Note that the computationally much slower discrete FT algorithm will not be able to accurately transform the non-equidistant data into the spectral domain. FFT packages for non-equidistantly sampled data exist today (see for example [Kunis Potts 2005]). Alternatively, another interpolation can be performed to force the interferogram onto an equidistant OPD grid.

4.2. Telescope compensation

SPIRE's first input port does not only receive radiation from an astronomical source but also from the telescope. In fact, the primary and secondary mirror of the Herschel telescope will be the main sources of power for all scientific observations. SCal can be used to add two additional sources with an approximate black body profile and ~ 2%/4% emissivity at temperatures up to ~ 100 K. The emission profiles of the telescope and SCal have to be determined and subtracted from any scientific measurements (see [Fischer et al. 2004] for a characterization of the emission of the Herschel mirror surface).

References

[Ade et al. 1999] “An Absolute Dual Beam Emission Spectrometer”. P.A.R. Ade, P.A. Hamilton, and D.A. Naylor. *FTS topical meeting, Santa Barbara*. Optical Society of America. Copyright © 1999 .

[Cooley Tukey 1965] “An algorithm for the machine calculation of complex Fourier series”. J.W. Cooley and J.W. Tukey. *Math.Comput.*. 19. 297-301. Copyright © 1965.

[Davis et al. 2001] *Fourier Transform Spectrometry*. S.P. Davis, M.C. Abrams, and J.W. Brault. Academic Press, San Diego. Copyright © 2001.

[Fischer et al. 2004] “Cryogenic far-infrared laser absorptivity measurements of the Herschel Space Observatory telescope mirror coatings”. J. Fischer, T. Klaassen, N. Hovenier, G. Jakob, A. Poglitsch, and O. Sternberg. *Applied Optics*. 43. 19. 3765-3771. Copyright © 2004.

[Frigo Johnson 2005] “The Design and Implementation of FFTW3”. M. Frigo and S. Johnson. *Proceedings of the IEEE*. 93. 2. 216-231. Copyright © 2005. *See also http://www.fftw.org/*.

[Kunis Potts 2005] *NFFT*. S. Kunis and D. Potts. *http://www.math.uni-luebeck.de/potts/nfft/*. Copyright © 2005.

[Swinyard et al. 2003] “The Imaging FTS for Herschel SPIRE”. B.M. Swinyard, K. Dohlen, D. Ferrand, J.-P. Baluteau, D. Pouliquen, P. Dargent, G. Michel, J. Martignac, P. Ade, P. Hargrave, M. Griffin, D. Jennings, and M. Caldwell. *Proceedings SPIE*. 4850. 698-709. Copyright © 2003.

[Tahic Naylor 2005] “Apodization Functions for Fourier Transform Spectroscopy”. M.K. Tahic and D.A. Naylor. *FTS topical meeting, Alexandria*. Optical Society of America. Copyright © 2005.